Marine Micropaleontology 195 (2025) 102451

Contents lists available at ScienceDirect

Marine Micropaleontology

journal homepage: www.elsevier.com/locate/marmicro

An integrative analysis of *Plectocapillus antarcticus* gen. et sp. nov. from Antarctica: Morphology, chemical composition, and phylogeny

Somin Lee [a], Michael A. Kaminski [b], Fabrizio Frontalini [c], Jisu Yeom [d], Nayeon Park [e], Wonchoel Lee [a,*]

[a] Department of Life Science, College of Natural Sciences, Hanyang University, 04763 Seoul, Republic of Korea
[b] Geosciences Department, King Fahd University of Petroleum & Minerals, PO Box 5070, Dhahran 31261, Saudi Arabia
[c] Department of Pure and Applied Sciences, Urbino University, 61029 Urbino, Italy
[d] Research Institute for Natural Sciences, Hanyang University, Seoul 04763, Republic of Korea
[e] Institute of Low Temperature Science, Hokkaido University, Sapporo 060-0819, Japan

ARTICLE INFO

Keywords:
Chemical composition
Diversity
DNA barcode
New genus
SEM-EDS
Taxonomy

ABSTRACT

In this study, *Plectocapillus antarcticus* gen. et sp. nov., belonging to the Family Pseudobolivinidae Wiesner, 1931, Superfamily Spiroplectamminoidea Cushman, 1927, was described from Maxwell Bay, King George Island, Antarctica. The species is distinguished by its elongate, slender, and entirely biserial test, fragile, thin agglutinated wall, a globular, organic proloculus, and the areal, rounded to arch-like aperture. Notably, this species previously assigned taxonomically as *Spiroplectammina filiformis* Earland, 1934 or *Textularia tenuissima* Earland, 1933, in nearby areas. However, morphological comparison revealed differences in chamber arrangement, biserial pair number, test width, and proloculus wall composition. SEM-DES analysis identified Al, Ca, Fe, Mg, Si, and Ti as major chemical elements present in the test wall, along with the traces of K, Mn, Na, P, Ce, Cl, F, S, Sr, and Zr. Phylogenetic analysis of partial SSU rRNA and mitochondrial COI gene sequences confirmed that *P. antarcticus* forms a well-supported clade, sister to *Spiroplectammina biformis*. The slender, flexible test, organic proloculus, and inclusion of heavy element-rich minerals suggests potential adaptation to hypoxic or interstitial habitats. By integrating morphological, chemical, and molecular data, this study contributes to the expanding fundamental database and understanding of Antarctic foraminiferal diversity and emphasizes the necessity for continued research in the region.

1. Introduction

West Antarctic is one of the regions on Earth that is highly impacted by climate (Davison et al., 2024). Rapid environmental variations due to climate change in the region have been reported, for instance, in the annual ice sheet loss that increased approximately three-fold from the year 1992 to 2017 (Shepherd et al., 2018). Furthermore, it is predicted that the West Antarctic ice-shelf melting will accelerate (Naughten et al., 2023) affecting terrestrial and marine biodiversity in the region (Lin et al., 2021; Lee et al., 2022; Strugnell et al., 2022). Therefore, ongoing biodiversity monitoring and research in the West Antarctic region is crucial to improve our understanding of the impact of environmental changes on biodiversity and to predict future trends and threats.

Studies on Antarctic foraminiferal diversity and distribution started from the nineteenth century (d'Orbigny, 1839; Brady, 1884) and numerous studies have been published up to date (Heron-Allen and Earland, 1922, 1932; Wiesner, 1931; Earland, 1933, 1934, 1936; Parr, 1950; Uchio, 1960; McKnight, 1962; Pflum, 1966; Kennett, 1967, 1968; Anderson, 1975; Osterman and Kellogg, 1979; Finger and Lipps, 1981; Milam and Anderson, 1981; Ward et al., 1987; Mackensen et al., 1990; Violanti, 1996; Mikhalevich, 2004; Majewski, 2005, 2010; Dejardin et al., 2018; Mikhalevich and Bozhenova, 2018; Majewski et al., 2023). However, research sites are concentrated in specific areas in the Antarctic regions, and morphological descriptions are commonly omitted leading to ambiguous species identifications. To improve the understanding of the Antarctic foraminiferal fauna, investigations of less-studied sites and taxonomical studies including re-examination of tentatively identified species are necessary. Referring to some recent studies, the Antarctic foraminiferal fauna shows a high degree of endemism and relatively high abundance-to-predominance of

* Corresponding author.
E-mail address: wlee@hanyang.ac.kr (W. Lee).

https://doi.org/10.1016/j.marmicro.2025.102451
Received 3 November 2024; Received in revised form 14 February 2025; Accepted 14 February 2025
Available online 17 February 2025

agglutinated taxa, due to the low water temperature and undersaturation of $CaCO_3$ (Mikhalevich, 2004). High taxonomic diversity and richness of monothalamous foraminifera (agglutinated or organic-walled, unilocular foraminifera) have been commonly reported in some Antarctic regions (Gooday et al., 1996; Pawlowski et al., 2002; Habura et al., 2004; Majewski et al., 2007), and several new foraminiferal taxa have been described, including: *Bowseria arctowskii* (Sinniger et al., 2008), *Crithionina delacai* (Gooday et al., 1995), *Notodendrodes hyalinosphaira* (De Laca et al., 2002), *Psammophaga magnetica* (Pawlowski and Majewski, 2011), and *Vellaria zucchellii* (Sabbatini et al., 2004). In the same context, during the 2021/2022 and 2022/2023 austral summer, we identified a new agglutinated foraminiferal genus, belonging to the Family Pseudobolivinidae Wiesner, 1931, Superfamily Spiroplectamminoidea Cushman, 1927, from Maxwell Bay, King George Island (West Antarctic).

The Family Pseudobolivinidae Wiesner, 1931 is one of the five extant families included in the Superfamily Spiroplectamminoidea Cushman, 1927. This family was originally established at the subfamily level, in association with the description of genus *Pseudobolivina* Wiesner, 1931. The type species, *Pseudobolivina antarctica*, was originally described as *Bolivina punctata* var. *arenacea* Heron-Allen & Earland, 1922, from Antarctic regions (Ellis and Messina, 1940 and later). Pseudobolivinidae can be distinguished from other families within Spiroplectamminoidea by the biserial to loosely biserial arrangement without a distinct initial planispiral stage and wedge-shaped chambers not strongly overhanging at the sides. On the other hand, since the morphological feature of biserial arrangement without a planispiral initial stage is inconsistent with the description of the Superfamily Spiroplectamminoidea in Loeblich and Tappan (1987), "*Test planispirally coiled in early stage; later biserial*", further examination of this group to emend the superfamily description or to make the Pseudobolivinidae an independent superfamily is needed. Presently, three extant genera – *Lacroixina* Saidova, 1981, *Parvigenerina* Vella, 1957 and *Pseudobolivina* Wiesner, 1931 – and nine extant species are included in the Family Pseudobolivinidae.

Here, we describe a new pseudobolivinid genus and a new species from Antarctica and provide plates including SEM and photomicrographs, as well as the chemical characterization of the dominant elements constituting the test identified by Scanning Electron Microscopy with Energy Dispersive X-ray Spectrometry (SEM-EDS) analysis, and the partial sequences from the mitochondrial COI (Cytochrome c Oxidase subunit I) and Small Subunit ribosomal RNA (SSU rRNA) genes.

2. Materials and methods

2.1. Sample collection

Field sampling was conducted in the two inlets of the Maxwell Bay, King George Island (Antarctica), during 2021/2022 and 2022/2023 austral summer (Fig. 1; Table 1). The sediment samples were collected by using van Veen grab sampler on a small vessel "Sejong I". The collected sediment was directly subsampled using an acrylic corer, or plastic spoons, and placed into 250 ml sample bottles. After arriving at the King Sejong Station, the samples were sieved through 63 μm or 38 μm sieves, fixed with 99 % EtOH, and stored at a temperature lower than −30 °C until transported to the biodiversity laboratory at the Hanyang University (South Korea).

2.2. Laboratory procedures and morphological analysis

In the laboratory, sediment samples from Marian Cove were dried at 55 °C in an oven before being observed under a stereomicroscope (Olympus SZX12), and the samples from Potter Cove were examined in wet conditions. Individuals of the new inferred genus were picked and preserved on a cardboard micropaleontology slide or 1.5 ml tube with 99 % EtOH. Photomicrographs of selected individuals were taken under multi-focus using a digital camera (Canon EOS 90D) attached to a stereomicroscope (Olympus SZX12), and the stacked images were obtained by Helicon Focus 7.6.4, software (Helicon Soft). Because of the fragile test, some specimens were mounted on glass slides with 70 % EtOH, temporally covered with cover glasses, and observed under a compound microscope (Olympus BX51TF). Photomicrography was also done with the temporal slides using the same digital camera attached to the optical stereomicroscopes. For more detailed morphological observation, some specimens were placed on SEM stubs, coated with gold in an ion coater (COXEM SPT-20), and examined under a SEM (COXEM EM30). Test size measurement was performed using the obtained photographs and Fiji software (Schindelin et al., 2012). Test length, maximum width, proloculus diameter were measured and the number of biserial chamber pairs

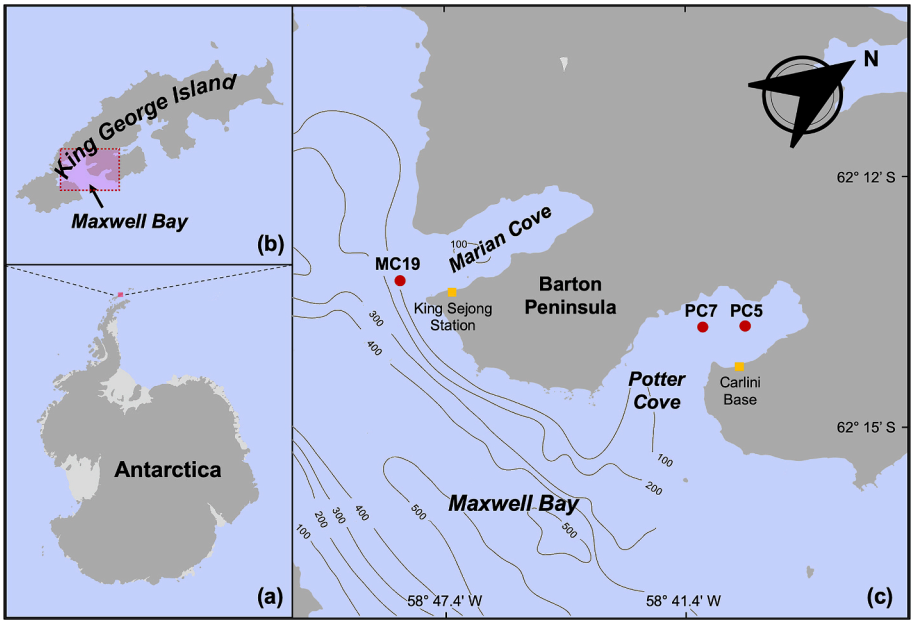

Fig. 1. Map showing the sample stations. (a) Map showing Antarctica, the purple dot indicates the location of King George Island, adjacent to the Antarctic peninsula; (b) Enlarged map of the purple dot in (a), showing King George Island. The location of Maxwell Bay is markd by a purple square; (c) Magnified map of Maxwell Bay, indicated by the purple square in (b). Sampling sites (MC19, PC5, and PC7) in Marian Cove and Potter Cove are marked with red dots.

Table 1
Sampling information including labels (PC: Potter Cove, MC: Marian Cove), geographical coordinates, date of sampling, method of sediment collection, temperature, and water depth.

Station	Lat. (S)	Long. (W)	Date	Equipment	Temp. (°C)	Depth (m)
PC5	62°13′48.29″	58°39′55.08″	2023.1.13.	van Veen Grab	1.7	43
PC7	62°13′48.64″	58°40′57.73″	2023.1.13.	van Veen Grab	1.7	30
MC19	62°13′14.88″	58°48′31.32″	2022.1.24.	van Veen Grab	1	102

were counted. Due to the common damage and deformation into irregular shapes, both Feret diameter and the minimal Feret diameter (minFeret) were measured for the proloculus, and the average values were calculated. Taxonomic classification was done based on Kaminski (2014), Loeblich and Tappan (1987), and the original descriptions of related taxa, collected in the online database, the Ellis and Messina Catalogue of Foraminifera (Ellis and Messina, 1940 and later).

Additionally, the EDS analyses were conducted to determine the major elements comprising the test wall. Four gold coated specimens used for SEM imaging were analyzed using a SEM (COXEM, EM30-AXN) equipped with Oxford AztecOne platform, at COXEM analysis center, Daejeon (South Korea). The measurement was carried out at an acceleration voltage of 20 kV. BSE (Backscattered electron) with images of the whole test were obtained at first, and then the EDS analysis. For some individuals, additional analyses were conducted by focusing on the middle part of test, apertural region, and the basal part around the proloculus.

2.3. DNA extraction, PCR amplification, and sequencing

Twenty-seven individuals isolated from station PC7 were used to extract DNA, with each extraction performed using a single individual. Prior to DNA extraction, 23 individuals photographed before extraction using a digital camera (Canon EOS 90D) attached stereomicroscope (Olympus SZX12) or compound microscope (Olympus BX51). gDNA was extracted referred to GITC* method (Weiner et al., 2016) or by using Qiagen DNeasy Blood and Tissue Kit and the manual provided by manufacturer with the reduced elution buffer volume (60 μl) at the final step. PCR amplification of partial COI (Leray COI fragment) and 3′ end partial SSU rRNA gene sequences were performed with the primers listed below (Table 2). MAXIME™ PCR PreMix i-Taq (iNtRON Biotechnology, Korea) was used to prepare the reaction mix, Ultra-Pure Water (WELGENE, Korea) 5–13 μl, forward primer (10 pMol/μl) 1 μl, reverse primer (10 pMol/μl) 1 μl and DNA template 1–5 μl were added to the reaction volume of 20 μl, referring to the manufacturer's guide. Clontech PCR Thermal Cycler GP (TaKaRa, Japan) was used for all PCR reactions, and the thermal cycle used for the COI fragment amplification was 2 min at 96 °C, followed by 40 cycles of 96 °C for 20 s, 50 °C for 30 s, 72 °C for 40 s, and the final extension 5 min at 72 °C. Sequences of the 3′ end region in SSU rRNA gene were amplified by nested PCR, with the primer pair s14F3-sB for the first PCR, and the second reaction was carried out with the primer pair S15r-NewR. PCR conditions were 2 min at 94 °C followed by 35 cycles of 94 °C for 20 s, 50 °C for 15 s, 68 °C for 90 s and the final elongation at 72 °C for 3 min. The secondary PCR was done under the same conditions as the first, with the annealing temperature of 52 °C and the cycle number 25. Amplification results were confirmed on 1.5 % agarose gels using 4 μl of each PCR product, then for the successful samples, purification and Sanger sequencing were performed using sequencing services provided by Bionics (Seoul, Korea). The obtained sequences were registered in the NCBI/GenBank database (accession nos. PQ810949-PQ810952 for SSU rRNA sequences; PQ811770-PQ811772 for the partial COI sequences).

Table 2
Primer sequences used for PCR amplification.

	Primer	Type	Sequence (5′ - 3′)	Reference
COI	Foraminifera_COI_fwd1	forward	GWG GWG TTA ATG CTG GTY GAAC	(Macher et al., 2021)
	Foraminifera_COI_rev	reverse	RWR CTT CWG GAT GWC TAA GAR ATC	
SSU rRNA	s14F3	forward	ACG CAA GTG TGA AAC TTG	(Pawlowski, 2000)
	sB	reverse	TGA TCC TTC TGC AGG TTC ACC TAC	
	S15r	forward	GTG GTG CAT GGC CGT	(Merkado et al., 2015)
	NewR	reverse	TTC ATC GGT AAG AGC GAC	

2.4. Phylogenetic analysis

Four newly obtained partial SSU rRNA gene sequences were aligned with 25 sequences retrieved from the GenBank database, including 22 sequences belonging to the Superfamily Spiroplectamminoidea, and three sequences of *Ammobaculites* selected as the outgroup. The multiple sequence alignment was performed using MUSCLE alignment tool with default option, as implemented in MEGA X software (Kumar et al., 2018). Phylogenetic trees were constructed using Maximum Likelihood (ML) method in the same software. The Hasegawa-Kishino-Yano (HKY; Hasegawa et al., 1985) model was selected as the substitution model, and Gamma distribution (+G) was selected for the among-site rate variation model, based on the result of the implemented model test. The relative measure of node support for the resulting trees were obtained as Bootstrap values (BVs) based on 1000 replicates. All positions with less than 95 % site coverage were eliminated using the partial deletion option, resulting in a dataset of 710 positions used for the analysis.

The newly obtained COI sequences were verified using Open Reading Frame Finder (ORFFinder), BLAST, and CD-Search tool based on Conserved Domain Database (CDD) of NCBI. The sequences were analyzed using ORF Finder with Genetic code 4 applied based on (Macher et al., 2021), to confirm the ORFs and Coding Sequences (CDSs). The resulting ORFs were then searched against the non-redundant (nr) protein sequences database using BLASTP to identify and validate the foraminiferal COI CDS. Additionally, the confirmed CDS were submitted to CD-Search tool to identify associated protein families and verify the functions of the Conserved Domains (CDs). Following verification, three newly obtained partial COI sequences were aligned with 13 sequences from GenBank encompassing all validated COI sequences available for agglutinated foraminiferal taxa at the time of analysis. Multiple sequence alignment of the 16 sequences was performed using the MUSCLE alignment tool with default settings in MEGA X software. Maximum Likelihood (ML) phylogenetic tree was constructed based on the dataset, with the HKY + I was selected as the substitution and among-site rate variation model, according to the implemented model test. BVs were based on 1000 replicates. Using the partial deletion option, all positions with less than 98 % site coverage were eliminated, resulting in a dataset of 308 sites for the analysis. The accession numbers of all sequences downloaded from GenBank were listed in the Supplementary data 1.

3. Results

3.1. Systematic Taxonomy

Phylum Foraminifera d'Orbigny, 1826.

Class Globothalamea Pawlowski, Holzmann & Tyszka, 2013.

Order Lituolida Lankester, 1885.

Suborder Spiroplectamminina Mikhalevich, 1992.

Superfamily Spiroplectamminoidea Cushman, 1927 **Emended.**

Test planispirally coiled in early stage, later biserial, or biserial throughout; agglutinated, non-canaliculate.

Remarks. To include the Family Pseudobolivinidae in the Superfamily Spiroplectamminoidea as Loeblich and Tappan (1987) and Kaminski (2014) suggest, the description of the Spiroplectamminoidea needs to be revised to include taxa with an entirely biserial chamber alignment. Therefore, a slight modification is made here, by adding the phrase '*or biserial throughout*'.

Family Pseudobolivinidae Wiesner, 1931.

Test biserial or loosely biserial with cuneate chambers in later stage; wall thin, agglutinated; aperture oval to rounded, single or multiple, areal to terminal and may be produced on a neck.

Plectocapillus Lee, Kaminski & Frontalini **gen. nov.**

Type species. *Plectocapillus antarcticus* gen. et sp. nov.

Derivation of name. Latin *plĕcto* (to plait, braid, interweave) + *căpíllus* (hair), meaning 'plaited hair'. Slender, flexible and biserial test is reminiscent of plaited hair.

Description. Test elongate, slender, flexible, and fragile. Chamber arrangement biserial throughout, with a tendency to become loosely biserial in the later part of the test. Aperture single, rounded to arch-like areal opening, slightly above the base of the apertural face. Wall finely agglutinated, except the proloculus, without agglutinated particles.

ZooBank registration. LSID: urn:lsid:zoobank.org:act:9E1BE047-BF99-4BEE-B329-392496FC9C85.

Remarks. Due to the wholly biserial test without an early spiral stage, and thin single-layered agglutinated wall without canaliculi, we placed this genus in the Family Pseudobolivinidae Wiesner, 1931. The Pseudobolivinidae currently includes three extant genera (i.e., *Lacroixina* Saidova 1981, *Parvigenerina* Vella, 1957 and *Pseudobolivina* Wiesner, 1931). The present genus differs from *Lacroixina* by the early chamber arrangement, and the apertural details. *Lacroixina* has streptospiral-like arrangement with two pairs of opposed chambers at the base in the microspheric generation, and a produced oval aperture on a neck. *Plectocapillus* has biserial chamber arrangement throughout, and a rounded to arch-shaped areal aperture without a neck. Meanwhile, *Plectocapillus* is similar to *Parvigenerina* by its biseriality, however, the latter has a distinct neck and a nearly rectilinear, uniserial chamber arrangement in the later stage. Additionally, the present genus differs from *Pseudobolivina* in having almost parallel sides, rather than a distinctly tapering aboral part with rapidly enlarging chambers. Despite belonging to a different family, Spiroplectamminidae Cushman, 1927, the megalospheric form of the genus *Palustrella* Brönnimann, Whittaker, & Zaninetti, 1992, is very similar to *Plectocapillus*, by having an entirely biserial chamber arrangement, gradually tapering width, and rounded periphery. However, *Palustrella* differs from *Plectocapillus* by having a planispiral early stage in the microspheric form, and its interiomarginal elongate arch-like equatorial aperture, rather than a rounded to arch-like areal aperture slightly above the basal margin of the final chamber. Likewise, *Morulaplecta Höglund, 1947* within the Family Spiroplectamminidae, is similar to *Plectocapillus* in possessing a non-agglutinated, proteinaceous bulbous proloculus. However, it is distinguished from *Plectocapillus* by its early streptospiral chamber arrangement, which completely encloses the proloculus.

Fig. 2. Photomicrographs of *Plectocapillus antarcticus* gen. et sp. nov. Scale is 100 µm, indicated at upper left. 1: Holotype (NIBRPR0000111310) from the station PC7, entire test view; 2: Paratype (NIBRPR0000111312) from PC5, entire test view, chambers are more separated than other specimens due to deformation during slide preparation; 3: Paratype (NIBRPR0000111313) from PC5, entire test view; 4: Paratype (NIBRPR0000111314) from PC5, entire test view, the lower part is bent and rotated (black triangle).

Plectocapillus antarcticus Lee, Kaminski & Frontalini **gen. et** sp. **nov. (**Figs. 2, 3**. 1–10; Supplementary data 2).**

Textularia tenuissima: Earland, 1934, p. 115. pl.10, fig. 22; Ishman and Domack, 1994, p. 153, pl. 1, Fig. 1; Majewski, 2010, p. 65, text Fig. 2–2.

Spiroplectammina filiformis: Rodrigues et al., 2010, p. 354, text Fig. 4b.

Materials examined. Total of 55 individuals; two from station MC19, seven from station PC5, 46 from station PC7. Two from MC19 and nine from PC7 for SEM, including one from MC19 and three from PC7 for EDS; seven from PC5, 10 from PC7 for photomicrography; 27 individuals from PC7 for DNA extraction, 23 individuals among DNA extracted individuals also morphologically examined by photomicrography.

Type material. Holotype (register no. NIBRPR0000111310) from Potter Cove, King George Island, station PC7, 62°13′48.64″ S, 58°40′57.73″ W, depth 30 m, collected by van Veen Grab, on 13 January 2023, preserved in 70 % EtOH due to highly delicate test. Four paratypes; register no. NIBRPR0000111311 from Marian Cove, King George Island, station MC19, 62°13′14.88″ S, 58°48′31.32″ W, water depth 102 m, collected by van Veen Grab, on 24 January 2022, mounted on a SEM stub and Au coated; register nos. NIBRPR0000111312-NIBRPR0000111314 from Potter Cove, King George Island, station PC5, 62°13′48.29″ S, 58°39′55.08″ W, depth 43 m, collected by van Veen Grab, on 13 January 2023, preserved in 70 % EtOH due to the highly delicate test to handle. All type specimens deposited in National Institute of Biological Resources (NIBR, South Korea).

Other materials. Five individuals were successfully sequenced among 27 DNA extracted individuals, two of which yielded both SSU rRNA and COI sequences, while the SSU rRNA sequence was obtained from two

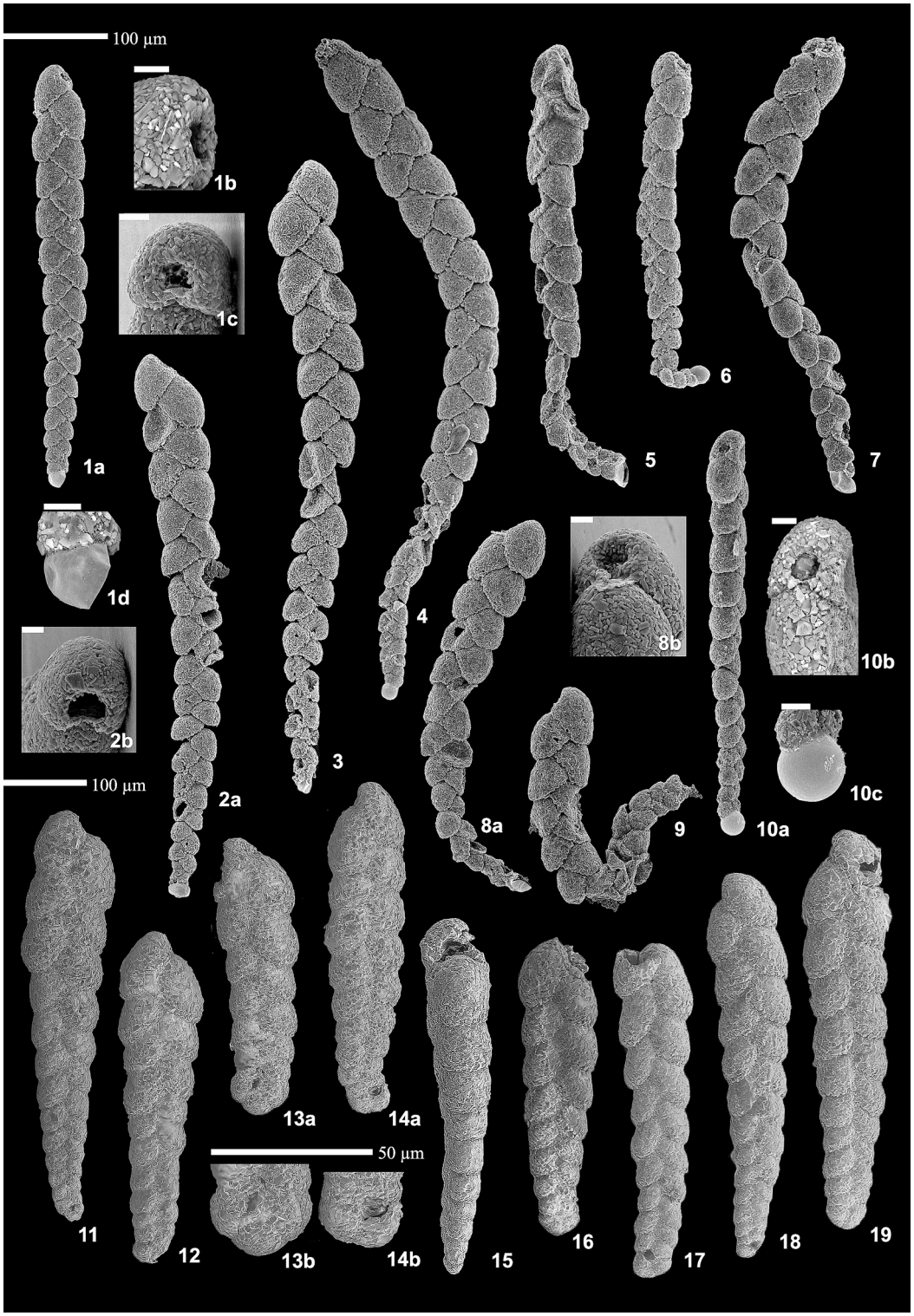

Fig. 3. SEM images of *Plectocapillus antarcticus* gen. et sp. nov. (1–10) and paratypes of *Textularia earlandi* (11–19). *T. earlandi* specimens are deposited in NHM London, Earland collection, Cabinet A30, slide ZF3518, from Discovery Station 144, South Georgia, depth 155–178 m. Scales are 100 mm unless otherwise explained, scale bar for *P. antarcticus* is at the top left and the scale bar for *T. earlandi* is at the middle left. 1: Paratype from MC19 (NIBRPR0000111311), (1a) entire test view, (1b) close-up of apertural part from BSE image, (1c) close-up of aperture at the apertural face, (1d) close-up of proloculus, from BSE image, scales of 1b–d are 10 mm, indicated at the top left of each image; 2a, 3–8a, 9, 10a: Entire test view of *P. antarcticus* specimens from PC7. Most of the tests are bent or curved, and some chambers are damaged or shrunken. Proloculus in 4, 5 and 8 are intact, 2a, 3, 6, 7, and 9a have damaged proloculus, and the proloculus of 9 is lost; 2b, 8b, 10b: Close-up of aperture, scales are 10 mm, indicated at the top left of each figure; 10c: close-up of proloculus, from BSE image, scale is 10 mm, at the top left; 11, 12, 13a, 14a, 16–19: Entire test view of *T. earlandi* paratype specimens, the apertural part of figure 17 damaged; 15: Peripheral view of *T. earlandi* specimen, the apertural part is damaged; 13b, 14b: Close-up of the early spiral arrangement, scale is 50 mm, indicated at the upper side of both images.

others and the COI sequence from the remaining one (GenBank accession nos. PQ810949-PQ810952 for SSU rRNA sequences; PQ811770-PQ811772 for the partial COI sequences).

Derivation of name. The specific name '*antarcticus*' corresponds to the Latinized 'Antarctic', in the masculine form according to the gender of the genus name '*Plectocapillus*' ('*căpíllus*' is masculine), because the type locality of the new species is in Antarctica.

ZooBank registration. LSID: urn:lsid:zoobank.org:act:579021CE-C0AE-4460-A98D-00F81BD750C7.

Description. Test slender, elongate, flexible and very delicate, easy to break; oval to rounded rectangular in section. Periphery bluntly rounded throughout, edge slightly straight in early portion, more lobulate in later portion. Chamber arrangement biserial throughout, later tending to become more loosely biserial than early part. Flexibility of the test causing some specimens to bend during sorting or observation process, resulting highly loose biserial appearance, as if each chamber about to separate. Chamber pair number ranging from 9 to 21, with an average of 14. Chambers cuneate, with round upper margins. Sutures distinct, straight, and oblique with respect to the central axis of the test from the proloculus to the final chamber. Aperture single, rounded to arch-like areal opening, on the apertural face, slightly above the basal border of the final chamber. Wall agglutinated, built of fine particles in a single layer, except the proloculus; particles agglutinated densely, cement material and type difficult to distinguish, no surface pores of calcitic cement observed. Proloculus globular, without agglutinated particles, transparent when observed under stereo- or compound-microscope in liquid fixative; the proloculus very fragile, only 18 of 51 examined individuals having intact globular proloculus, the rest with broken initial end or shrunken proloculus. Surface smooth, silvery to grayish in color, occasionally black and white colored particles included, under stereomicroscope; under compound microscope, test dark gray to slightly brownish with darker agglutinated particles more distinctly visible. Test length about 212 to 676 μm, with average of 414 μm; width 42 to 81 μm, average 59 μm; average proloculus diameter 9 to 25 μm, with an average of 20 μm (Supplementary data 3).

Remarks. Due to the flexibility and fragility of the test, damage, or deformation such as shrinkage of chambers, bending and stretching of test occurs very easily, changes in the size and shape of the apertural part and proloculus has been frequently observed (Fig. 3.1–10).

In several genera and species belonging to Spiroplectamminoidea, both megalospheric and microspheric forms have been described, differing in the presence or absence of an early spiral arrangement (Supplementary data 4). In contrast, in this new species, all observed specimens exhibit a fully biserial arrangement, with no evidence of alternation of generations with early spiral coiling. There is another possibility that two generations distinguishable by differences in proloculus diameter and test size may exist, however, further examination of larger sample data is necessary to verify the statistical significance.

This species has previously been recorded as slender variety of *Textularia tenuissima* or *Spiroplectammina filiformis* in marine areas around the Antarctic Peninsula and the South Shetland Islands (Earland, 1934; Ishman and Domack, 1994; Majewski, 2010; Rodrigues et al., 2010). However, the specimens figured in these references mostly have damaged initial ends, and the morphological description were omitted. Based on the figures, the specimens show greater similarity to the current new species than the original descriptions of the assigned species, in terms of chamber shape and degree of the test tapering.

Referred to the original description, *S. filiformis* has a spiral coil in early stage of both the megalo- and microspheric forms and has 6 to 10 pairs of chambers in the biserial part (Earland, 1934). The present new species has a greater number of chamber pairs with an average of 14, and an initial spiral coil is not observed in any of the examined specimens.

Textularia tenuissima is originally described from South Georgia and Antarctic regions by Earland (Earland, 1933) and due to the preoccupancy of the name, it was later renamed *T. earlandi*, by Parker (1952). The morphological characteristics of *T. earlandi* - fragile, elongate, straight to curved test; a single layered thin wall of light gray to silver in color; little sign of interstitial cement - is very similar to *P. antarcticus.* The range of proloculus diameter recorded in the original description of *T. earlandi* also almost the same as in *P. antarcticus*: proloculus diameter of 8–24 (*T. earlandi*) vs. 9–25 (*P. antarcticus*). However, these species can be distinguished by several characteristics: the number of chamber pairs, test length, presence of an initial spiral, the proloculus, and aperture morphology. *Textularia earlandi* has an entirely agglutinated test, and trimorphic form, with two megalospheric forms, A1, A2, and a microspheric form, B. A1 has a shorter test and large neatly rounded initial spire. A2 has almost acutely pointed apex with an equally long test, and in some cases, no initial spire. B has an acute apex and usually no initial coil, but some B forms were reported as with complete initial coil (Earland, 1933). However, the initial spiral arrangement in *P. antarcticus* is not present. Additionally, the chamber pair number, test length is much higher and longer in *P. antarcticus* than in *T. earlandi*: the chamber pair number of 5.5–12 (*T. earlandi*) vs. 9–21 (*P. antarcticus,* average 14); length of 184–500 (*T. earlandi*) vs. 212–676 (*P. antarcticus,* average 414). The described width (breadth) of *T. earlandi* is wider than that of *P. antarcticus*: 52–100 (*T. earlandi*) vs. 42–81 (*P. antarcticus,* average 59). Meanwhile, there is no mention of a naked proloculus in the description of *T. earlandi*, but *P. antarcticus* has non-agglutinated proloculus. The apertural details of both species are also different: the new species has an aerial opening, while *T. earlandi* has a curved slit on the inner edge of final chamber. The differences between these species are confirmed by the SEM images of '*T. tenuissima'* type slide (ZF 3518) deposited in the NHM London, Earland collection (Fig. 3. 11–19).

Distribution. Antarctic regions close to the Western Antarctic Peninsula.

This study: Maxwell Bay (King George Is.).

Records from previous studies presumed to be misidentified (Earland, 1934; Ishman and Domack, 1994; Majewski, 2005, 2010; Rodrigues et al., 2010): Port Lockroy (Wiencke Is.) off Adelaide Is., Bransfield Strait, Admiralty Bay (King George Is.), Maxwell Bay (King George Is.), Flandres Bay, Andvord Bay, Marguerite Bay, off Anvers Is., Andvord Bay, off Brabant Is., Flandres Bay, off Kyiv Peninsula, Beascochea Bay, off Davis Coast, Cierva Cove, Brialmont Cove). The detailed distributional records and map indicating the recorded locations are presented in the supplementary data 5.

3.2. Test chemical composition

The main elements constituting the test wall were determined through SEM-EDS analysis with four specimens in the Fig. 3 (no. 1, 2, 7, 10). The results of the entire test surface revealed that aluminum (Al), calcium (Ca), iron (Fe), oxygen (O), silicon (Si), and titanium (Ti) were commonly detected with similar weigth percent (wt%) in the entire test surface mapping of all specimens (Table 3; Fig. 4; Supplementary data 6). Magnesium (Mg) was detected only in the specimen Fig. 3–1 as the lowest wt% (0.39 %). However, subsequent analyses on magnified regions within other specimens confirmed the presence of Mg, which was consistently identified as one of the elements with the lowest wt% (Table 3; Supplementary data 6). The signal of carbon (C) detected with

Table 3
Weight % of main constituent elements identified from EDS analysis of the entire test, magnified parts and points on the proloculus.

Analyzed part	Specimen	Al	C	Ca	Fe	K	Mg	Mn	Na	O	P	Si	Ti
Entire test	Fig. 3–1	0.85	64.25	2.68	2.6		0.39			27.87		0.95	0.42
	Fig. 3–2	0.76	64.74	2.08	3.35					27.51		0.97	0.59
	Fig. 3–**7**	0.92	64.66	2.42	3.2					27.31		0.99	0.51
	Fig. 3–**10**	0.61	67.92	1.65	3.21					25.4		0.71	0.49
Apertural part	Fig. 3–1	1.92	47.54	7	5.78	0.15	0.97			31.58	1.04	2.88	1.13
	Fig. 3–2	1.77	48.43	5.56	7.68		0.71			30.93	0.68	2.92	1.32
	Fig. 3–**10**	1.39	54.91	5.32	7.38		0.65			26.44	0.25	2.53	1.14
Middle part of test	Fig. 3–1	3.14	32.08	9.47	10.28	0.24	1.4		0.39	34.74	1.32	4.68	2.26
	Fig. 3–**7**	3.05	33.49	10.14	11.34	0.32	1.05	0.27		32.02	1.58	4.7	2.03
Basal end	Fig. 3–1	1.27	58.37	3.68	5.13		0.56			27.91	0.26	1.86	0.95
	Fig. 3–**7**	0.92	64.44	3.38	5.66	0.17	0.28			23.04		1.3	0.8
	Fig. 3–**10**	0.61	65.89	2.19	5.04		0.25		0.29	24.05		0.87	0.8
Proloculus (point analysis)	Fig. 3–1	2.32	50.82	1.48	4.01		0.78			37.91		2.68	
	Fig. 3–**7**		45.42	7.85	5.06	1.74				37.44	2.5		
	Fig. 3–**10**	0.54	57.27	2.08	5.34				1.6	32.73		0.45	

the highest wt% in the entire test surface analysis of all examined specimens. However, the majority of the detected C originate from the background carbon tape (Fig. 4; Supplementary data 6). Based on the mapping results, most detected elements exhibit uniform distribution across the entire surface with relatively consistent intensity, excluding the proloculus. In the case of Ti, certain particles exhibited distinctly higher signal intensities than those detected in the surrounding areas. The proloculus region exhibited generally lower intensities for all detected elements compared to other parts on the test (Fig. 4; Supplementary data 6).

Analysis on the magnified area of the middle, aperture, and basal end of the test detected additional elements: potassium (K), manganese (Mn), sodium (Na), and phosphorus (P). The wt% of these elements were found to be among the lowest (Table 3). The main elemental composition and distribution of the magnified regions were consistent with those observed in the entire test surface mapping results. Additionally, the particles containing certain elements at high wt% were observed more distinctly in the magnified mapping results, indicating enrichment of these elements within specific grains (Fig. 4; Supplementary data 6).

The point analysis performed on several distinguishable particles observed in the BSE images also identified additional elements, indicating the presence of particles containing these elements (Supplementary data 6): cerium (Ce), chlorine (Cl), fluorine (F), sulfur (S), strontium (Sr), and zirconium (Zr). Point analysis of the proloculus region detected the presence of C, O, Fe, Si, Al, Ca, Mg, Na, P, and K (Table 3). The elements C, O, Fe, and Ca were consistently detected across all three points. At each measured point, C and O exhibited the highest wt%, collectively accounting for approximately 83–90 %. Variations were observed in the presence of other elements, along with slight differences in their wt%. Ti, one of the main elements detected from tests, was not detected in all three points.

3.3. Phylogenetic analysis

The DNA extraction and PCR amplification successfully yielded either SSU rDNA or COI sequences from a total of five specimens. Among them, both SSU rDNA and COI sequences were successfully obtained from two specimens, only SSU rDNA sequences were amplified from two others, and only the COI sequence was amplified from a single specimen. The newly obtained 3′ end partial SSU rDNA sequences of *P. antarcticus* comprise 790–969 nt (872 nt in average), and the GC content ranges 39.2–40.5 % (39.7 % in average). The partial COI sequences comprise 342–356 nt (347 nt in average), and GC content ranges 26.6–27.5 % (26.9 % in average). The CDS of partial COI gene comprise 312–324 nt, and the GC content ranges 26.0–26.2 %. The obtained COI sequences were analyzed using ORF Finder, which identified three potential ORF candidates for each sequence. BLAST analysis of these candidates revealed that only one ORF in each sequence corresponded to the foraminiferal COI. The CDS corresponding to this ORF was further analyzed using the CD-search tool, which confirmed that the conserved domains of these CDSs belong to the Heme-copper oxidase subunit I superfamily (CDD accession no. cl00275) and match the cytochrome oxidase subunit 1 (CDD accession no. cd01663) group.

In the MLtree of partial SSU rRNA gene sequences, all included genera except *Spiroplectammina* spp., form well-supported clades (BV = 99, 100 %). *Plectocapillus antarcticus,* forming a well-supported (BV = 99 %) clade, branches within a group (BV = 74 %) consisting of two sister clades: one including *Spiroplectammina* spp. clade (1) and *Spirotextularia* spp., without significant BV support, and the other group (BV = 99 %) of *Spiroplectammina* spp. clade (2) and *P. antarcticus. Nouria polymorphinoides* branches at the base of the two-sister clade containing group (BV = 100 %). *Spiroplectammina* represents polyphyletic groups, with the clade (1) forming a sister clade with *Spirotextularia* spp., another genus of Spiroplectamminidae, and the clade (2) with *P. antarcticus*, which results in the Family Spiroplectamminidae appearing paraphyletic in the tree.

In the MLtree of partial COI sequences, *Plectocapillus antarcticus* forms a well-supported clade (BV = 99 %), and branches with *Spiroplectammina* sp. (BV = 95 %). The tree basically consists of two clades, one of the Suborder Xenophyophoroidea Lister, 1909 (*Bizarria bryiformis, Psammina limbata,* and *Aschemonella monilis*) and the other clade including other agglutinated taxa, which is not well supported (BV < 70 %). The latter clade includes two relatively well-supported subclades, one with monothalamiids (*Micrometula* sp. and *Psammophaga* sp., BV = 76 %) and the other consisting of taxa of the class Globothalamea (BV = 99 %). The Globothalamea clade groups taxa belonging to the order Lituolida (*Plectocapillus antarcticus, Spiroplectammina* sp., *Trochammina hadai, Eggerelloides scaber, Entzia macrescens,* and *Cribrostomoides* sp.) and Textulariida (*Cyrea szymborska* and *Textularia pseudogramen*), and both of which appear to be paraphyletic.

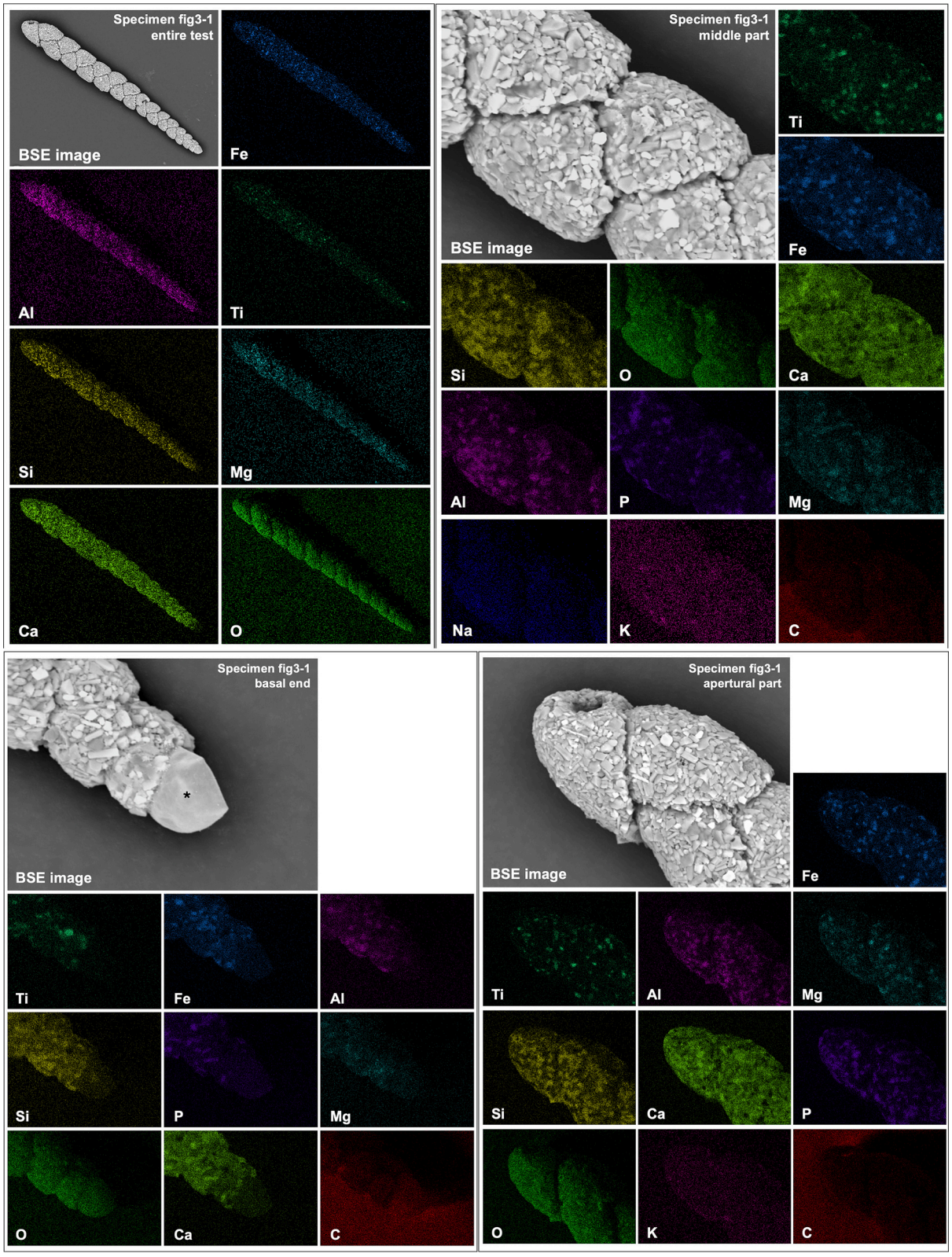

Fig. 4. BSE and major element mapping images obtained from SEM-EDS analysis of the specimen in figure3-1. The type of element is indicated at the bottom left of each mapping image, and the distribution of the elements is indicated by color, with the intensity of the color corresponding to the intensity of the detected signal. The (*) symbol is indicating the point analysis performed spot.

4. Discussion

4.1. Distribution and ecology

As outlined in the remarks in the systematic taxonomy section, *P. antarcticus* has previously been assigned as other species by various authors. Based on existing records including images of specimens presumed to represent *P. antarcticus*, it is confirmed to have a wide distribution across the coastal waters, adjacent seas, and nearby islands of Western Antarctic Peninsula (Supplementary data 5). According to the previous records and this study, *P. antarcticus* may also exhibit a broad bathymetric range, occurring at depths from 47 m (Admiralty Bay; Majewski, 2005, 2010) to 2200 m (Bransfield Strait; Ishman and Domack, 1994). Such a wide bathymetric distribution is one of the common peculiar features observed in benthic foraminiferal assemblages from Antarctic waters (Mikhalevich, 2004). However, it is simultaneously necessary to re-examine the voucher specimens in previous records to verify whether they are all taxonomically consistent with *P. antarcticus* or represent a mixed species complex. Furthermore, additional sampling in the region to collect sufficient specimens, followed by morphological and molecular analyses, would enhance our understanding of the wide depth range of *P. antarcticus*.

Unfortunately, the vertical distributional pattern in sediment layer or mode of life of *P. antarcticus* was not examined in this study. Based on the elongate, biserial test morphology, this species may however be able to penetrate the sediment layers and adaptive to low-oxygen conditions. Slender, elongate, and serial (uni-, bi-, or tri-) morphotypes of foraminifera are common and adapted to low-oxygen environments, and reported to dwell as epifauna in low-oxygen waters or as infauna in well-oxygenated environments (Kaiho, 1994; Bernhard and Sen Gupta, 1999; Mancin et al., 2013; Nwojiji et al., 2019). Test structures of such morphotypes exhibit high surface area to volume ratio that can enhance the efficiency of protoplasmic mixing between the inner and outer parts of the shell, thereby decreasing metabolic activity within the cell, and lower the oxygen and nutrient requirements of the organism. Similarly, the slender elongated body form is a convergent trend in interstitial meiofauna, which enhances mobility, adhesion, and anchoring in habitats of small dimension while promoting substance absorption and diffusion within the body through an increased surface-to-diameter ratio (Giere, 2009). Therefore, the test morphology of *P. antarcticus* also seems to be advantageous in hypoxic conditions at bathyal depths and in an interstitial habitat. Future physiological studies within their cytoplasm, as well as the behavioral responses of living individuals, and sediment depth-specific sampling could further enhance our understanding of the life strategy of the species within the sediment.

4.2. Flexible test wall and organic proloculus

Plectocapillus antarcticus possesses a thin, delicate, test wall which is flexible when wet. Generally, a flexible test wall is uncommon in multilocular agglutinated group and is mainly observed in monothalamous taxa (Bender, 1995). Among the multilocular agglutinated group, the genus *Leptohalysis* Loeblich and Tappan, 1984, which belongs to the Family Reophacidae, Suborder Hormosinina, has been described as possessing a flexible test when wet (Chaster, 1892; Höglund, 1947; Loeblich and Tappan, 1984; Bell, 1996). It has a slender, elongate test, and uniserial chamber arrangement. In particular, the test of *L. catella* (Höglund, 1947) is described as exhibiting test wall similar with *P. antarcticus*: thin and delicate, with small polyhedral particles arranged edge to edge, attached to an inner lining. Although no detailed studies have been conducted on the evolutionary or ecological significance of the flexible test in these taxa, the observed similarities between their tests suggest that the combination of a thin delicate test wall, a slender, elongate, and segmented (serial) body may be the factors contributing to this flexibility.

The transparent, rounded proloculus predominantly composed organic materials, is another distinctive characteristic of *Plectocapillus*. Such proloculus type has been reported in a few multichambered agglutinated taxa: *Morulaplecta* (Höglund, 1947), *Cyrea* (Holzmann et al., 2018), *Leptohalysis* (Loeblich and Tappan, 1984; Kitazato et al., 2009). The proloculus of *Morulaplecta* and *Cyrea* are covered by subsequent chambers. In contrast, the photomicrographs of *Leptohalysis kaikoi* (Kitazato et al., 2009) reveal an exposed, smooth, rounded, naked proloculus closely resembling that of *P. antarcticus*. In detail, *L. kaikoi* has been described as predominantly composed of organic matter, with some mineral grains very sparsely distributed. Furthermore, EDS analysis of the proloculus detected the signals of Si, Al, Mg, Ca, and Fe, which were interpreted as originating from those mineral grains. The EDS point analysis of the *Plectocapillus'* proloculus also reveals the presence of the same types of elements, with C and O detected at significantly high concentrations, accounting for 83–90 wt% in total (Table 3). This suggests that the proloculus is mainly composed of organic material, and the detected inorganic elements may originate from incorporated mineral particles, as proposed for *L. kaikoi* (Kitazato et al., 2009). Alternatively, certain elements, such as Fe or Ca, may be biologically bound to organic components through biomineralization (Hedley, 1963; Bertram and Cowen, 1998). However, further biochemical studies, including mass spectrometry, are required to precisely determine the components of the proloculus.

The evolutionary and biological significance of the flexible test and organic proloculus in multilocular agglutinated foraminifera remains poorly understood. In meiofauna, a flexible body is known to represent a convergent trend as an adaptation for survival in interstitial habitats. In particular, a rugged body enhances articulation and increases the number of segments, resulting in a flexible, vermiform morphology (Giere, 2009). At the same time, the flexible body can reduce drag in strong currents within epibenthic habitats (Levinton, 2009). In this respect, segmentation through serially arranged chambers in *Plectocapillus* and *Leptohalysis* may contribute to the test flexibility. For instance, *L. scotti* has been reported to inhabit both epifaunal and infaunal environments (Ernst et al., 2000; Gustafsson and Nordberg, 2001), and its flexible test is possibly advantageous for survival in these habitats. At the same time, thin foraminiferal test wall may enhance material exchange efficiency in low-oxygen environments (Kaiho, 1994; Ni et al., 2024). Therefore, the thin-walled proloculus in *Plectocapillus* may be also related to high metabolic efficiency, which could be advantageous for the survival of juveniles in such environments.

Further ecological and biological investigations with a greater number of taxa exhibiting these traits will provide clearer insights into such characteristics. Continuous taxonomic investigations and surveys of unexplored regions are necessary to discover additional taxa with similar test wall and proloculus.

4.3. Test wall composition

The EDS analysis revealed the main elemental composition (Al, Ca, Fe, Mg, O, Si, Ti) and distribution in both the overall structure and magnified regions of *P. antarcticus*. Additionally, point analysis provides the chemical composition of certain distinct particles in the test. The detected elements are consistent with previously reported elements in the environments adjacent to the present study area (Yeo et al., 2004; Jerosch et al., 2018). Based on relevant literatures including previous studies analyzing the test mineral composition of agglutinated taxa (Jeong and Yoon, 2002; Armynot du Châtelet et al., 2013; Capotondi et al., 2019; Mohan and Kumari, 2021), approximate mineral groups of the analyzed particles were broadly inferred: carbonates, phosphates (apatite), Fe- or Ti-rich oxides, silicates, and zircon. Additionally, some grains exhibited elemental compositions of complexity with relatively high wt% of Al, suggesting either the presence of mixed mineral phases or clay minerals including aluminosilicates with the incorporation of several elements as impurities (Fig. 4; Supplementary data 6).

Unfortunately, research on the mineral composition of surface

sediments in the study area is highly limited, restricting its use as additional supporting evidence for the mineral assignment in this study. The component of benthic sediment or even biochemical component of benthic organisms in the study area is however known to be influenced by terrestrial, lithogenic particles transported by glaciomarine sedimentation processes (Ahn et al., 1996; Chang and Yoon, 2000; Abele et al., 2008; López-Martínez et al., 2012). Therefore, mineralogical characters and tectonic settings of the surrounding terrestrial environment (e.g., Barton Peninsula) are additionally considered. The source rocks of Barton Peninsula mainly consist of volcanic rock and plutonic rock. Notably, various minerals derived from source rocks and their alternation minerals have been reported in the sediments of adjacent terrains: Fe-rich smectite, kaolinite, illite, chlorite, quartz, plagioclase, amphibole, mica, zeolite, pyrite, halite, gypsum, pyrophyllite, carbonate minerals, Ti- and Fe-oxides, magnetite, and zircon (Cox et al., 1980; Willan and Armstrong, 2002; Lee et al., 2004; Hauck et al., 2012; Jung et al., 2017; Lee et al., 2019). These minerals are consistent with those inferred in the test particles of *P. antarcticus*.

Previous studies have been reported the accumulation of Fe-, Ti- or Zr-rich heavy mineral particles in the test wall or in the cytoplasm of other taxa, including *Bathysiphon, Psammophaga*, *Reophax, Textularia,* and *Agglutinella* (Cole and Valentine, 2006; Makled and Langer, 2010; Pawlowski and Majewski, 2011; Sabbatini et al., 2016; Capotondi et al., 2019; Garrison, 2019). The physicochemical properties (electron density and polarity) of such minerals are possible to form chemical bondings with biological structures composing the foraminiferal pseudopodia or test cement materials (Makled and Langer, 2010; Pawlowski and Majewski, 2011; Sabbatini et al., 2016). Such features have been suggested to be related to the mineral selection mechanism, and to enhance the physical stability of the test, thereby enhancing protection against predation (Langer et al., 1995) and environments characterized by high wave or current agitation (Capotondi et al., 2019; Garrison, 2019). Additionally, the heavy minerals in monothalamiids have been suggested to contribute to buoyancy regulation, thereby enabling the individuals to anchor more efficiently within the sediment (Nyholm, 1957; Dahlgren, 1962; Pawlowski and Majewski, 2011; Sabbatini et al., 2016). Therefore, Fe-, Ti-rich and zircon mineral particles in the test of *Plectocapillus* possibly contribute to the structural stability of its delicate, flexible test to penetrate the sediment, or to survive in environments subject to disturbances such as glacier erosion or seasonal influx of detrital materials.

Further crystallographic studies using X-ray diffraction (XRD) and Raman spectroscopy are expected to enable more precise mineral identification of both the test of *P. antarcticus* and surrounding seafloor sediments. Additionally, quantitative assessment and comparison of the morphological and compositional diversity of the particles constituting tests and the sediment will provide insights into the particle selectivity of *P. antarcticus* in the environment. Furthermore, integrating physiological and ecological examinations on the species would enhance the understanding of adaptive mechanisms in response to specific environments.

4.4. Phylogenetic relationships

In this study, we obtained the 3′ end SSU rRNA and Leroy COI gene fragment sequences of a newly discovered Antarctic agglutinated foraminifera. Phylogenetic analysis confirms that these sequences form a monophyletic group distinct from other related agglutinated genera. Consequently, this work contributes to the expansion of foraminiferal reference sequence data, by providing verified DNA sequences for two molecular markers, accompanied by species-level taxonomic classification and detailed morphological descriptions. Notably, foraminiferal COI sequences were first reported as recently as 2021, with research initially focusing on calcareous LBF species (Macher et al., 2021; Girard et al., 2022), thereby limiting the availability of validated Spiroplectamminoidea sequences on GenBank to just one at the time of analysis for this study. By contributing to the expansion of the foraminiferal reference sequence database, this study ultimately enhances the

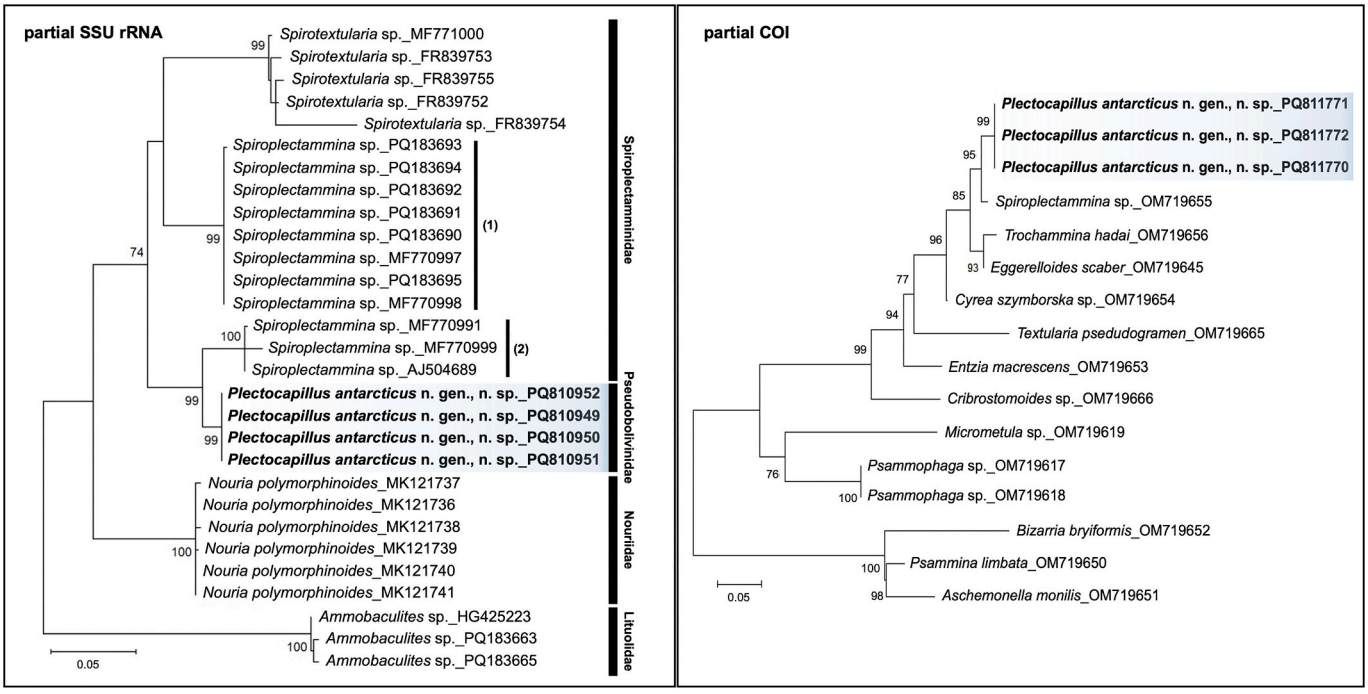

Fig. 5. Maximum Likelihood (ML) phylogenetic trees inferred from the partial SSU rRNA and COI gene sequences of *Plectocapillus antarcticus* gen. et sp. nov., and other agglutinated taxa. Bootstrap values (BV) > 70 % are shown at the nodes, and the trees are unrooted. Sequences indicated in bold are newly obtained in this study. The accession numbers are indicated next to the underscore (_) symbol following each taxon name. The numbers in brackets - (1), (2) - for *Spiroplectammina* sp. in the SSU rRNA tree are added to distinguish different clades. The taxon names at the right end of the SSU rRNA tree represent the families of taxa included in each black bar region.

resolution of research utilizing the database, such as species diversity assessments and environmental monitoring through Next-Generation Sequencing (NGS) techniques (e. g., eDNA metabarcoding).

The phylogenetic analysis revealed that, in the SSU rRNA ML tree, *Spiroplectammina* sp. appeared paraphyletic, unlike other genera (Fig. 5). Clade (2) formed a sister group with *P. antarctica* rather than being branched within the Family Spiroplectamminidae. Notably, all specimens of clade (2) were collected from the Arctic Svalbard (Holzmann et al., 2024). They may represent Arctic endemic taxa that is not part of the Family Spiroplectamminidae. Further collection of the specimens and detailed morphological analyses is essential to validate this hypothesis. An alternative possibility is that the entire branches, including *Spirotextularia* sp., *Spiroplectammina* sp., clades (1) and (2), and *P. antarcticus*, belongs to Spiroplectamminidae. However, under this scenario, *Plectocapillus*, which does not exhibit the early spiral chamber arrangement, would be included in Spiroplectamminidae, leading to a conflict with the traditional morphological classification criteria (see the Supplementary data 4). On the other hand, it may be attributed to the limited dataset used for the analysis, as numerous taxa within Spiroplectamminoidea were missing from the reference database. At the time of the analysis, SSU rRNA gene sequences were available for only two families and three genera out of the five families and 16 genera within Spiroplectamminoidea, while COI sequences were available for only one genus (*Spiroplectammina*). Furthermore, as shown in the Fig. 5, many of the data entries lacked species-level identification. Enhancing both the quality and quantity of database would improve the resolution of phylogenetic relationships.

Such discrepancies between morphological classification and molecular phylogeny have been reported across multilocular agglutinated foraminifera. Recent molecular phylogenetic studies have suggested that multilocular agglutinated taxa are paraphyletic, and the monophyly of orders (Lituolida, Loftusiida, Textulariida) proposed by Loeblich and Tappan (Loeblich and Tappan, 1989) has not been confirmed. Furthermore, most clades, aside from a few genera, have not been well-supported (Pawlowski et al., 2013; Holzmann et al., 2018). Hence, the precise molecular phylogenetic position of *P. antarcticus* remains unclear and requires cautious interpretation. Alternatively, we primarily classified *P. antarcticus* within the Order Lituolida, Superfamily Spiroplectamminoidea, and Family Pseudobolivinidae, based on the Kaminski (2014) classification. Simultaneously, molecular phylogeny for the SSU rRNA sequences was performed using GenBank-registered sequences assigned to Spiroplectamminoidea under the same classification, rather than including all the taxa assigned as "Textulariida" in Pawlowski et al. (2013).

Therefore, expansion of molecular datasets along with precise morphological identification is essential to resolve the molecular phylogenetic relationships across multilocular agglutinated taxa. Additionally, further integrative studies on the candidates of phenotypes that reflect the evolutionary relationships of foraminifera, such as test organic linings (Tyszka et al., 2021) and wall ultrastructure (Dubicka, 2019), would significantly help resolve inconsistencies between morphological classification and molecular phylogeny, and advance our understanding of the evolutionary relationships of this group.

5. Conclusion

A new genus and species, *Plectocapillus antarcticus,* belonging to the Order Lituolida, Family Pseudobolivinidae, was described from King George Island (West Antarctica). The entire biseriality, organic proloculus, flexible, fragile test, and the areal aperture are the distinguishable characteristics. SEM-EDS analysis revealed major elements constituting the test surface: Al, Ca, Fe, Mg, O, Si, and Ti. The molecular phylogeny with partial SSU rRNA gene and partial COI sequences of *P. antarcticus* revealed a well-supported clade, sister to *Spiroplectammina biformis* (Spiroplectamminidae). Due to insufficient reference sequences and the problem of inconsistency between molecular and morphological phylogenies in multilocular agglutinated foraminifera, the position of *Plectocapillus* remains unresolved. Further molecular and morphological studies including more taxa within the Superfamily Spiroplectamminoidea are necessary to reveal the phylogenetic relationships. The slender, flexible test, organic proloculus wall, and chamber arrangement suggest possible adaptations to hypoxic conditions and interstitial habitats, warranting further ecological and physiological investigations. In this regard, this study contributes to expanding the foundational dataset on extant foraminifera, and improving the understanding of Antarctic biodiversity, by providing morphological and molecular data on the newly discovered taxon. Furthermore, by describing a new species and genus, we emphasize the necessity of additional exploration in this region.

Funding

This research was supported by Korea Polar Research Institute (KOPRI), grant number PE23900, National Institute of Biological Resources (NIBR), funded by the Ministry of Environment (MOE) of the Republic of Korea, grant number NIBRE202402, and Basic Science Research Program through the National Research Foundation of Korea (NRF) funded by the Ministry of Education, grant number 2021R1I1A2043807. This research was supported by Korea Basic Science Institute (National research Facilities and Equipment Center) grant funded by the Ministry of Education (2023R1A6C101A009).

CRediT authorship contribution statement

Somin Lee: Writing – original draft, Visualization, Methodology, Investigation, Conceptualization. **Michael A. Kaminski:** Writing – review & editing, Resources, Methodology, Conceptualization. **Fabrizio Frontalini:** Writing – review & editing, Supervision, Conceptualization. **Jisu Yeom:** Writing – review & editing, Resources, Investigation. **Nayeon Park:** Writing – review & editing, Resources, Investigation. **Wonchoel Lee:** Writing – review & editing, Supervision, Conceptualization.

Declaration of competing interest

The authors declare that they have no known competing financial interests or personal relationships that could have appeared to influence the work reported in this paper.

Acknowledgements

We would like to express sincere gratitude to the 2021/2022 and 2022/2023 summer research team and the 35th and 36th overwintering teams at the King Sejong Station, Antarctica. Special thanks go to Dr. Sun-Yong Ha's research team, the overwintering crews of marine research, mechanic, and the maritime safety officers, without whom the sampling would not have been possible. Additionally, we are grateful to KOPRI, for providing an invaluable opportunity to participate in field research in Antarctica. We also extend our sincere gratitude to Dr. Giles Miller, for providing images that allowed us to examine the type specimens of *T. tenuissima* at the Natural History Museum, London.

Appendix A. Supplementary data

Supplementary data to this article can be found online at https://doi.org/10.1016/j.marmicro.2025.102451.

Data availability

Data will be made available on request.

References

Abele, D., Atencio, A., Dick, D., Gonzalez, O., Kriews, M., Meyer, S., Philipp, E., Stölting, I., 2008. Iron, copper and manganese discharge from glacial melting into Potter Cove and metal concentrations in Laternula elliptica shells. In: The Antarctic ecosystem of Potter Cove, King-George Island (Isla 25 de Mayo), 39.

Ahn, I.-Y., Lee, S.H., Kim, K.T., Shim, J.H., Kim, D.-Y., 1996. Baseline heavy metal concentrations in the Antarctic clam, Laternula elliptica in Maxwell Bay, King George Island, Antarctica. Mar. Pollut. Bull. 32, 592–598.

Anderson, J.B., 1975. Ecology and Distribution of Foraminifera in the Weddell Sea of Antarctica. Micropaleontology 21, 69–96.

Armynot du Châtelet, E., Frontalini, F., Guillot, F., Recourt, P., Ventalon, S., 2013. Surface analysis of agglutinated benthic foraminifera through ESEM–EDS and Raman analyses: An expeditious approach for tracing mineral diversity. Mar. Micropaleontol. 105, 18–29.

Bell, K.N., 1996. Foraminiferan faunas of the Tamar River and Port Dalrymple, Tasmania : a preliminary study. Queen Victoria Museum and Art Gallery, Launceston, Tas.

Bender, H., 1995. Test structure and classification in agglutinated foraminifera. In: Kaminski, M., Geroch, S., Gasinski, M. (Eds.), Proceedings of the Fourth International Workshop on Agglutinated Foraminifera. Grzybowski Foundation Special Publication, pp. 27–70.

Bernhard, J.M., Sen Gupta, B.K., 1999. Foraminifera of oxygen-depleted environments. In: Sen Gupta, B.K. (Ed.), Modern Foraminifera. Springer Netherlands, Dordrecht.

Bertram, M.A., Cowen, J.P., 1998. Biomineralization in agglutinating foraminifera: An analytical SEM investigation of external wall composition in three small test forms. Aquat. Geochem. 4, 455–468.

Brady, H.B., 1884. Report on the Foraminifera dredged by HMS Challenger, during the years 1873–1876. Reports of the scientific results of the voyage of HMS challenger. Zoology 9, 1–184.

Capotondi, L., Mancin, N., Cesari, V., Dinelli, E., Ravaioli, M., Riminucci, F., 2019. Recent agglutinated foraminifera from the North Adriatic Sea: What the agglutinated tests can tell. Mar. Micropaleontol. 147, 25–42.

Chang, S.-K., Yoon, H.-I., 2000. Holocene glaciomarine sedimentation in Marian Cove, King George Island, West Antarctica. J. Korean Earth Sci. Soc. 21, 276–286.

Chaster, G.W., 1892. Report upon the foraminifera of the Southport Society of Natural Science district. First Report Southport Soc. Nat. Sci. 54–72.

Cole, K.E., Valentine, A.M., 2006. Titanium biomaterials: titania needles in the test of the foraminiferan Bathysiphon argenteus. Dalton Trans. 430–432.

Cox, C., Ciocanelea, R., Pride, D., 1980. Genesis of mineralization associated with Andean intrusions, northern Antarctic Peninsula region. Antarct. J. US 15, 22–23.

Dahlgren, L., 1962. Allogromia crystallifera n. sp., a monothalamous foraminifer. Zool. Bidrag från Uppsala 35, 451–455.

Davison, B.J., Hogg, A.E., Moffat, C., Meredith, M.P., Wallis, B.J., 2024. Widespread increase in discharge from west Antarctic Peninsula glaciers since 2018. Cryosphere 18, 3237–3251.

Dejardin, R., Kender, S., Allen, C.S., Leng, M.J., Swann, G.E.A., Peck, V.L., 2018. "Live" (stained) benthic foraminiferal living depths, stable isotopes, and taxonomy offshore South Georgia, Southern Ocean: implications for calcification depths. J. Micropalaeontol. 37, 25–71.

DeLaca, T.E., Bernhard, J.M., Reilly, A.A., Bowser, S.S., 2002. *Notodendrodes hyalinosphaira*(sp. nov.): Structure and autecology of an allogromiid-like agglutinated Foraminifer. J. Foraminifer. Res. 32, 177–187.

d'Orbigny, A.D., 1839. Voyage dans l'Amérique Méridionale. Foraminifères.

Dubicka, Z., 2019. Chamber arrangement versus wall structure in the high-rank phylogenetic classification of Foraminifera. Acta Palaeontol. Pol. 64, 1–18.

Earland, A., 1933. Foraminifera, Part II. Cambridge University Press, London, South Georgia.

Earland, A., 1934. Foraminifera, Part III, The Falklands sector of the Antarctic (excluding South Georgia). Cambridge University Press, London.

Earland, A., 1936. Foraminifera, Part IV. Additional records from the Weddell Sea sector from material obtained by the S.Y 'Scotia'. Cambridge University Press, London.

Ellis, B.F., Messina, A.R., 1940. and later. Catalogue of Foraminifera, Ellis and Messina catalogues of micropaleontology. The American Museum of Natural History, New York.

Ernst, S., Duijnstee, I., Jannink, N., van der Zwaan, B., 2000. An experimental mesocosm study of microhabitat preferences and mobility in benthic foraminifera: Preliminary results. In: Hart, M.B., Kaminski, M.A., Smart, C.W. (Eds.), Proceedings of the Fifth International Workshop on Agglutinated Foraminifera, 7. Grzybowski Foundation Special Publication, pp. 101–104.

Finger, K.L., Lipps, J.H., 1981. Foraminiferal Decimation and Repopulation in an Active Volcanic Caldera, Deception Island, Antarctica. Micropaleontology 27, 111–139. https://doi.org/10.2307/1485283.

Garrison, T.F., 2019. The microscopic mineral collector of the sea: *Agglutinella kaminskii* n.sp., a new benthic foraminifera from the Arabian Gulf. Micropaleontology 65, 277–283.

Giere, O., 2009. Biological Characteristics of Meiofauna, Meiobenthology: The Microscopic Motile Fauna of Aquatic Sediments. Springer, Berlin Heidelberg, Berlin, Heidelberg, pp. 87–102.

Girard, E.B., Langerak, A., Jompa, J., Wangensteen, O.S., Macher, J.-N., Renema, W., 2022. Mitochondrial Cytochrome Oxidase Subunit 1: A Promising Molecular Marker for Species Identification in Foraminifera. Front. Mar. Sci. 9, 809659.

Gooday, A.J., Bernhard, J.M., Bowser, S.S., 1995. The taxonomy and ecology of *Crithionina delacai* sp. nov., and abundant large agglutinated foraminifer from Explorers Cove. Antarct. J. Foraminifer. Res. 25, 290–298.

Gooday, A.J., Bowser, S.S., Bernhard, J.M., 1996. Benthic foraminiferal assemblages in Explorers Cove, Antarctica: A shallow-water site with deep-sea characteristics. Prog. Oceanogr. 37, 117–166.

Gustafsson, M., Nordberg, K., 2001. Living (stained) benthic foraminiferal response to primary production and hydrography in the deepest part of the Gullmar Fjord, Swedish west coast, with comparisons to Höglund's 1927 material. J. Foraminifer. Res. 31, 2–11.

Habura, A., Pawlowski, J., Hanes, S.D., Bowser, S.S., 2004. Unexpected foraminiferal diversity revealed by small-subunit rDNA analysis of Antarctic sediment. J. Eukaryot. Microbiol. 51, 173–179.

Hasegawa, M., Kishino, H., Yano, T.A., 1985. Dating of the human ape splitting by a molecular clock of mitochondrial-DNA. J. Mol. Evol. 22, 160–174.

Hauck, J., Gerdes, D., Hillenbrand, C.-D., Hoppema, M., Kuhn, G., Nehrke, G., Völker, C., Wolf-Gladrow, D.A., 2012. Distribution and mineralogy of carbonate sediments on Antarctic shelves. J. Mar. Syst. 90, 77–87.

Hedley, R.H., 1963. Cement and Iron in the Arenaceous Foraminifera. Micropaleontology 9, 433–441.

Heron-Allen, E., Earland, A., 1922. British Antarctic ("Terra Nova") Expedition, 1910. Natural History Report. Protozoa. Part II – Foraminifera, British Museum (Natural History), London.

Heron-Allen, E., Earland, A., 1932. Foraminifera; Part 1 The ice-free area of the Falkland Islands and adjacent seas. Cambridge University Press, London.

Höglund, H., 1947. Foraminifera in the Gullmar Fjord and the Skagerak. Appelbergs Boktryckeri, Uppsala.

Holzmann, M., Rigaud, S., Amini, S., Voltski, I., Pawlowski, J., 2018. *Cyrea Szymborska* gen. et sp. nov., a new textulariid foraminifer from the Mediterranean Sea. J. Foraminifer. Res. 48, 156–163.

Holzmann, M., Nguyen, N.-L., Angeles, I.B., Pawlowski, J., 2024. BFR2: a curated ribosomal reference dataset for benthic foraminifera. Sci. Data 11, 1292.

Ishman, S.E., Domack, E.W., 1994. Oceanographic controls on benthic foraminifers from the Bellingshausen margin of the Antarctic Peninsula. Mar. Micropaleontol. 24, 119–155.

Jeong, G., Yoon, H., 2002. Mineralogical characteristics and origins of smectite in the marine sediments around South Shetland Islands, Antarctica. J. Miner. Soc. Korea 15, 22–32.

Jerosch, K., Pehlke, H., Monien, P., Scharf, F., Weber, L., Kuhn, G., Braun, M.H., Abele, D., 2018. Benthic meltwater fjord habitats formed by rapid glacier recession on King George Island, Antarctica. Philos. Trans. R. Soc. A Math. Phys. Eng. Sci. 376, 20170178.

Jung, J., Koo, T., Yang, K., Kim, J., 2017. Mineralogical and geochemical characteristics of soils of Barton Peninsula, King George Island, South Shetland Islands, West Antarctica. J. Mineral. Soci. Korea 30, 21–29.

Kaiho, K., 1994. Benthic foraminiferal dissolved-oxygen index and dissolved-oxygen levels in the modern ocean. Geology 22, 719–722.

Kaminski, M.A., 2014. The year 2010 classification of the agglutinated foraminifera. Micropaleontology 60, 89–108.

Kennett, J.P., 1967. New foraminifera from the Ross Sea, Antarctica. Contribut. Cushman Foundat. Foraminiferal Res. 18, 133–135.

Kennett, J.P., 1968. The Fauna of the Ross Sea, Part 6, Ecology and Distribution of Foraminifera. R.E. Owen, Goverment Printer, Wellington, New Zealand.

Kitazato, H., Uematsui, K., Todo, Y., Gooday, A.J., 2009. New species of *Leptohalysis* (Rhizaria, Foraminifera) from an extreme hadal site in the western Pacific Ocean. Zootaxa 2059, 23–32-23–32.

Kumar, S., Stecher, G., Li, M., Knyaz, C., Tamura, K., 2018. MEGA X: Molecular Evolutionary Genetics Analysis across Computing Platforms. Mol. Biol. Evol. 35, 1547–1549.

Langer, M.R., Lipps, J.H., Moreno, G., 1995. Predation on foraminifera by the dentaliid deep-sea scaphopod *Fissidentalium megathyris*. Deep-Sea Res. I Oceanogr. Res. Pap. 42, 849–857.

Lee, Y.I., Lim, H.S., Yoon, H.I., 2004. Geochemistry of soils of King George Island, South Shetland Islands, West Antarctica: Implications for pedogenesis in cold polar regions. Geochim. Cosmochim. Acta 68, 4319–4333.

Lee, Y.I., Choi, T., Lim, H.S., 2019. Petrological and geochemical compositions of beach sands of the Barton and Weaver peninsulas of King George Island, West Antarctica: implications for provenance and depositional history. Int. Union of Geol. Sci. 42, 149–164.

Lee, J.R., Waterman, M.J., Shaw, J.D., Bergstrom, D.M., Lynch, H.J., Wall, D.H., Robinson, S.A., 2022. Islands in the ice: Potential impacts of habitat transformation on Antarctic biodiversity. Glob. Chang. Biol. 28, 5865–5880.

Levinton, J.S., 2009. Benthic life habits. In: Marine biology: function, biodiversity, ecology, 3 ed. Oxford University Press, New York.

Lin, Y., Moreno, C., Marchetti, A., Ducklow, H., Schofield, O., Delage, E., Meredith, M., Li, Z., Eveillard, D., Chaffron, S., Cassar, N., 2021. Decline in plankton diversity and carbon flux with reduced sea ice extent along the Western Antarctic Peninsula. Nat. Commun. 12, 4948.

Loeblich Jr., A.R., Tappan, H., 1987. Foraminiferal genera and their classification. Van Nostrand Reinhold Co., New York.

Loeblich, A.R., Tappan, H., 1984. Some New Proteinaceous and Agglutinated Genera of Foraminiferida. J. Paleontol. 58, 1158–1163.

Loeblich, A.R., Tappan, H., 1989. Implications of wall composition and structure in agglutinated foraminifers. J. Paleontol. 63, 769–777.

López-Martínez, J., Serrano, E., Schmid, T., Mink, S., Linés, C., 2012. Periglacial processes and landforms in the South Shetland Islands (northern Antarctic Peninsula region). Geomorphology 155-156, 62–79.

Macher, J.-N., Wideman, J.G., Girard, E.B., Langerak, A., Duijm, E., Jompa, J., Sadekov, A., Vos, R., Wissels, R., Renema, W., 2021. First report of mitochondrial COI in foraminifera and implications for DNA barcoding. Sci. Rep. 11, 22165.
Mackensen, A., Grobe, H., Kuhn, G., Fütterer, D.K., 1990. Benthic foraminiferal assemblages from the eastern Weddell Sea between 68 and 73°S: Distribution, ecology and fossilization potential. Mar. Micropaleontol. 16, 241–283.
Majewski, W., 2005. Benthic foraminiferal communities: distribution and ecology in Admiralty Bay, King George Island, West Antarctica. Polish Polar Res. 26, 159–214.
Majewski, W., 2010. Benthic foraminifera from West Antarctic fiord environments: An overview. Polish Polar Res. 31, 61–82.
Majewski, W., Lecroq, B., Sinniger, F., Pawłowski, J., 2007. Monothalamous foraminifera from Admiralty Bay, King George Island, West Antarctica. Polish Polar Res. 28, 187–210.
Majewski, W., Szczuciński, W., Gooday, A.J., 2023. Unique benthic foraminiferal communities (stained) in diverse environments of sub-Antarctic fjords, South Georgia. Biogeosciences 20, 523–544.
Makled, W.A., Langer, M.R., 2010. Preferential selection of titanium-bearing minerals in agglutinated Foraminifera: Ilmenite (FeTiO3) in *Textularia hauerii* d'Orbigny from the Bazaruto Archipelago, Mozambique. Rev. Micropaleontol. 53, 163–173.
Mancin, N., Hayward, B.W., Trattenero, I., Cobianchi, M., Lupi, C., 2013. Can the morphology of deep-sea benthic foraminifera reveal what caused their extinction during the mid-Pleistocene Climate Transition? Mar. Micropaleontol. 104, 53–70.
McKnight Jr., W.M., 1962. The distribution of foraminifera off parts of the Antarctic coast. Paleontological Research Institution, Ithaca, New York.
Merkado, G., Titelboim, D., Hyams-Kaphzan, O., Holzmann, M., Pawlowski, J., Almogi-Labin, A., Abdu, U., Herut, B., Abramovich, S., 2015. Molecular phylogeny and ecology of *Textularia agglutinans* d'Orbigny from the Mediterranean Coast of Israel: A case of a successful new incumbent. PLoS One 10, e0142263.
Mikhalevich, V.I., 2004. The general aspects of the distribution of Antarctic foraminifera. Micropaleontology 50, 179–194.
Mikhalevich, V.I., Bozhenova, O.V., 2018. Foraminifera from the 58th and 59th Russian Antarctic Expeditions, 2013–2014. Micropaleontology 64, 527–534.
Milam, R.W., Anderson, J.B., 1981. Distribution and Ecology of Recent Benthonic Foraminifera of the Adelie-George-V Continental-Shelf and Slope, Antarctica. Mar. Micropaleontol. 6, 297–325.
Mohan, C., Kumari, N., 2021. Basics of clay minerals and their characteristic properties. In: Do Nascimento, G.M. (Ed.), Clay and Clay Minerals. IntechOpen, Rijeka.
Naughten, K.A., Holland, P.R., De Rydt, J., 2023. Unavoidable future increase in West Antarctic ice-shelf melting over the twenty-first century. Nat. Clim. Chang. 13, 1222–1228.
Ni, S., Müter, D., Charrieau, L.M., Pirzamanbein, B., Choquel, C., Knudsen, K.L., Seidenkrantz, M.-S., Filipsson, H.L., 2024. Morphological insights from benthic foraminifera for environmental conditions in the Baltic Sea during the Last Interglacial. Authorea Preprints.
Nwojiji, C., Caswell, B., Marret, F., 2019. The PETM Extreme Climate Impact on the Benthic Foraminiferal Traits and Ecological Functioning in the Tropical Pacific Ocean. J. Ocean Res. 4, 6–19.
Nyholm, K.-G., 1957. Orientation and binding power of recent monothalamous foraminifera in soft sediments. Micropaleontology 3, 75–76.
Osterman, L.E., Kellogg, T.B., 1979. Recent benthic foraminiferal distributions from the Ross Sea, Antarctica; relation to ecologic and oceanographic conditions. J. Foraminifer. Res. 9, 250–269.
Parker, F.L., 1952. Foraminiferal distribution in the Long Island Sound - Buzzards Bay area.
Parr, W.J., 1950. Part 6 Foraminifera. B.A.N.Z.A.R. Expedition Committee, Adelaide.
Pawlowski, J., 2000. Introduction to the Molecular Systematics of Foraminifera. Micropaleontology 46, 1–12.
Pawlowski, J., Majewski, W., 2011. Magnetite-bearing foraminifera from Admiralty Bay, West Antarctica, with description of *Psammophaga magnetica*, sp. nov. J. Foraminifer. Res. 41, 3–13.
Pawlowski, J., Fahrni, J.F., Brykczynska, U., Habura, A., Bowser, S.S., 2002. Molecular data reveal high taxonomic diversity of allogromiid Foraminifera in Explorers Cove (McMurdo Sound, Antarctica). Polar Biol. 25, 96–105.
Pawlowski, J., Holzmann, M., Tyszka, J., 2013. New supraordinal classification of Foraminifera: Molecules meet morphology. Mar. Micropaleontol. 100, 1–10.
Pflum, C.E., 1966. The distribution of foraminifera in the eastern Ross Sea, Amundsen Sea, and Bellingshausen Sea, Antarctica. Paleontological Research Institution, Ithaca, New York.
Rodrigues, A.R., Maluf, J.C.C., Braga, E.D.S., Eichler, B.B., 2010. Recent benthic foraminiferal distribution and related environmental factors in Ezcurra Inlet, King George Island, Antarctica. Antarct. Sci. 22, 343–360.
Sabbatini, A., Pawlowski, J., Gooday, A.J., Piraino, S., Bowser, S.S., Morigi, C., Negri, A., 2004. *Vellaria zucchellii* sp. nov. a new monothalamous foraminifer from Terra Nova Bay, Antarctica. Antarct. Sci. 16, 307–312.
Sabbatini, A., Negri, A., Bartolini, A., Morigi, C., Boudouma, O., Dinelli, E., Florindo, F., Galeazzi, R., Holzmann, M., Lurcock, P.C., Massaccesi, L., Pawlowski, J., Rocchi, S., 2016. Selective zircon accumulation in a new benthic foraminifer, *Psammophaga zirconia*, sp. nov. Geobiology 14, 404–416.
Schindelin, J., Arganda-Carreras, I., Frise, E., Kaynig, V., Longair, M., Pietzsch, T., Preibisch, S., Rueden, C., Saalfeld, S., Schmid, B., Tinevez, J.-Y., White, D.J., Hartenstein, V., Eliceiri, K., Tomancak, P., Cardona, A., 2012. Fiji: an open-source platform for biological-image analysis. Nat. Methods 9, 676–682.
Shepherd, A., Ivins, E., Rignot, E., Smith, B., van den Broeke, M., Velicogna, I., Whitehouse, P., Briggs, K., Joughin, I., Krinner, G., Nowicki, S., Payne, T., Scambos, T., Schlegel .G., N.A, Agosta, C., Ahlstrøm, A., Babonis, G., Barletta, V., Blazquez, A., Bonin, J., Csatho, B., Cullather, R., Felikson, D., Fettweis, X., Forsberg, R., Gallee, H., Gardner, A., Gilbert, L., Groh, A., Gunter, B., Hanna, E., Harig, C., Helm, V., Horvath, A., Horwath, M., Khan, S., Kjeldsen, K.K., Konrad, H., Langen, P., Lecavalier, B., Loomis, B., Luthcke, S., McMillan, M., Melini, D., Mernild, S., Mohajerani, Y., Moore, P., Mouginot, J., Moyano, G., Muir, A., Nagler, T., Nield, G., Nilsson, J., Noel, B., Otosaka, I., Pattle, M.E., Peltier, W.R., Pie, N., Rietbroek, R., Rott, H., Sandberg-Sørensen, L., Sasgen, I., Save, H., Scheuchl, B., Schrama, E., Schröder, L., Seo, K.-W., Simonsen, S., Slater, T., Spada, G., Sutterley, T., Talpe, M., Tarasov, L., van de Berg, W.J., van der Wal, W., van Wessem, M., Vishwakarma, B.D., Wiese, D., Wouters, B., The, I.t, 2018. Mass balance of the Antarctic Ice Sheet from 1992 to 2017. Nature 558, 219–222.
Sinniger, F., Lecroq, B., Majewski, W., Pawłowski, J., 2008. *Bowseria arctowskii* gen. et sp. nov., new monothalamous foraminiferan from the Southern Ocean. Polish Polar Res. 29, 5–15.
Strugnell, J.M., McGregor, H.V., Wilson, N.G., Meredith, K.T., Chown, S.L., Lau, S.C.Y., Robinson, S.A., Saunders, K.M., 2022. Emerging biological archives can reveal ecological and climatic change in Antarctica. Glob. Chang. Biol. 28, 6483–6508.
Tyszka, J., Godos, K., Goleń, J., Radmacher, W., 2021. Foraminiferal organic linings: Functional and phylogenetic challenges. Earth Sci. Rev. 220, 103726.
Uchio, T., 1960. Benthonic foraminifera of the Antarctic Ocean. Seto Marine Biological Laboratory, Sirahama, Wakayama-ken, Japan.
Violanti, D., 1996. Taxonomy and distribution of recent benthic foraminifers from Terra Nova Bay (Ross Sea, Antarctica), Oceanographic Campaign 1987/1988. Paleontographia Italica 83, 25–71.
Ward, B.L., Barrett, P.J., Vella, P., 1987. Distribution and ecology of benthic foraminifera in McMurdo Sound, Antarctica. Palaeogeogr. Palaeoclimatol. Palaeoecol. 58, 139–153.
Weiner, A.K.M., Morard, R., Weinkauf, M.F.G., Darling, K.F., André, A., Quillévéré, F., Ujiie, Y., Douady, C.J., de Vargas, C., Kucera, M., 2016. Methodology for single-cell genetic analysis of planktonic foraminifera for studies of protist diversity and evolution. Front. Mar. Sci. 3, 255.
Wiesner, H., 1931. Die Foraminiferen der deutschen Südpolar Expedition 1901-1903. De Gruyter, Berlin.
Willan, R.C.R., Armstrong, D.C., 2002. Successive geothermal, volcanic-hydrothermal and contact-metasomatic events in Cenozoic volcanic-arc basalts, South Shetland Islands, Antarctica. Geol. Mag. 139, 209–231.
Yeo, J.P., Lee, J.I., Hur, S.D., Choi, B.-G., 2004. Geochemistry of volcanic rocks in Barton and Weaver peninsulas, King George Island, Antarctica: Implications for arc maturity and correlation with fossilized volcanic centers. Geosci. J. 8, 11–25.